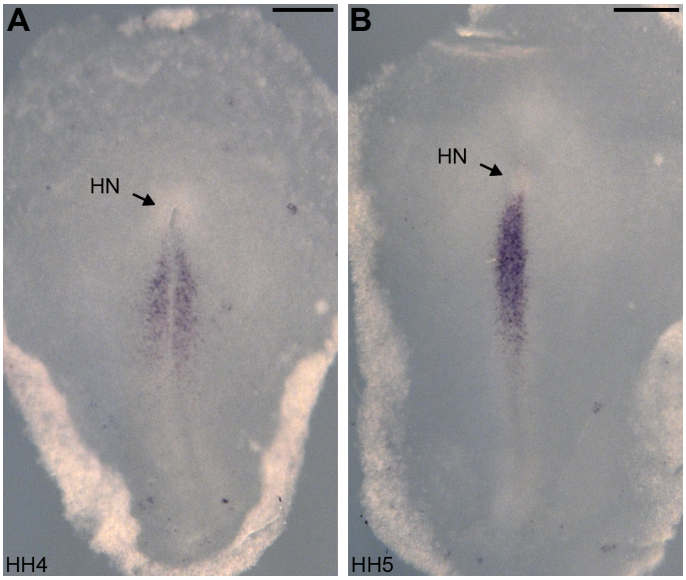

Figure S1. Expression of *LTK* in gastrula stages. (A-B) *In situ* hybridization of stage HH4 (A) and HH5 (B) embryos showing that *LTK* expression during gastrulation restricted to cells adjacent to the primitive streak, posterior to the Hensen's node (arrows), and absent in the neural plate and neural plate border. HN: Hensen's node. Scale bars: 200 μm.

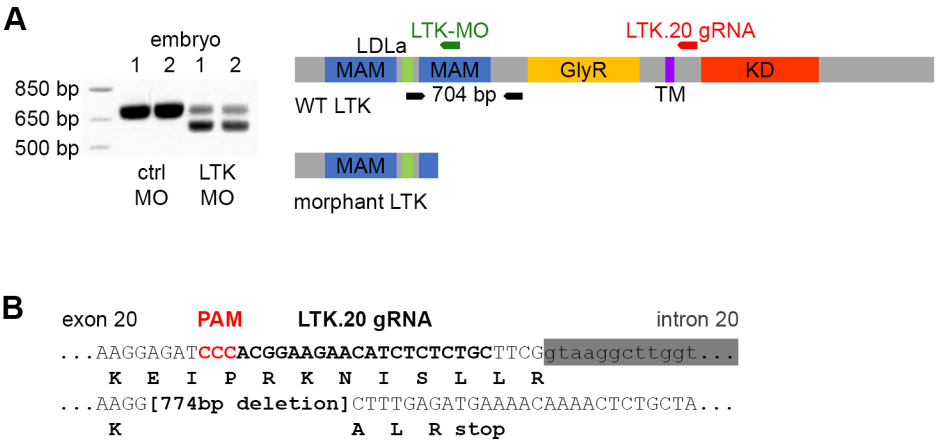

Figure S2. Validation of LTK loss-of-function reagents. (A) Gel image showing RT-PCR products obtained after electroporation of control or splice-blocking LTK MO. The lateral diagram shows the LTK protein domain structure and positions of LTK MO and primers used. Sequencing of the amplified region, containing the target exon8/intron8 junction, confirmed absence of exon 8 in the smaller PCR product obtained from LTK-depleted embryos. (B) Sequence of a cloned PCR product obtained from genomic DNA of Cas9-DF1 cells (Gandhi et al., 2017) transfection with LTK gRNA (LTK.20), showing a deletion event of 774 bp that caused a frame-shift posterior to the transmembrane domain predicting translation of a membrane localized putative dominant-negative.

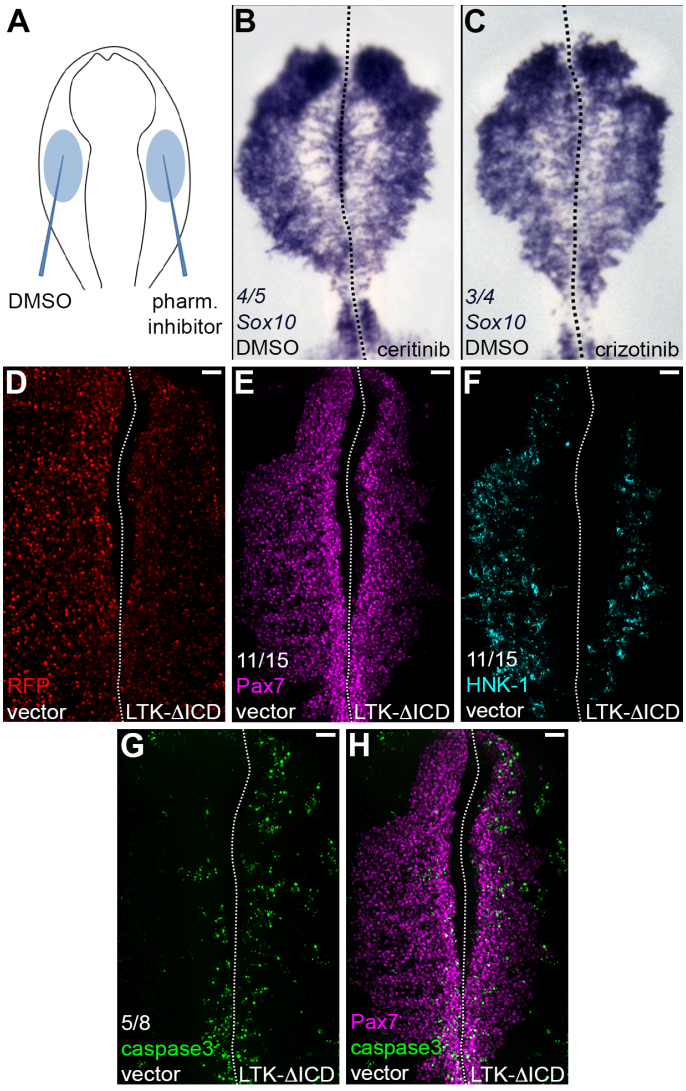

Figure S3. Pharmacological inhibitors and a putative dominant-negative for LTK impair neural crest migration. (A) Diagram showing strategy for injection of pharmacological inhibitors into the right-side head mesenchyme of HH9 embryos. (B-C) *In situ* hybridization for *Sox10* 10 h after unilateral injection of crizotininb (4 out of 5 embryos) (B) or ceritinib (3 out of 4 embryos) (C), showing reduced distance migrated by the cranial neural crest in comparison to the control side injected with DMSO vehicle alone. (D-F) Immunostaining of HH10 embryos after unilateral electroporation of V5-LTK-ΔICD showing reduced distance migrated by $Pax7^{+}$ cells (11 out of 15 embryos) (E), reduced expression of HNK-1 (11 out of 15 embryos) (F) and increased levels of cleaved caspase3 (G) (5 out of 8 embryos) amongst the neural crest population (H). RFP reporter was electroporated on both sides (D). Scale bars: 50 μm.

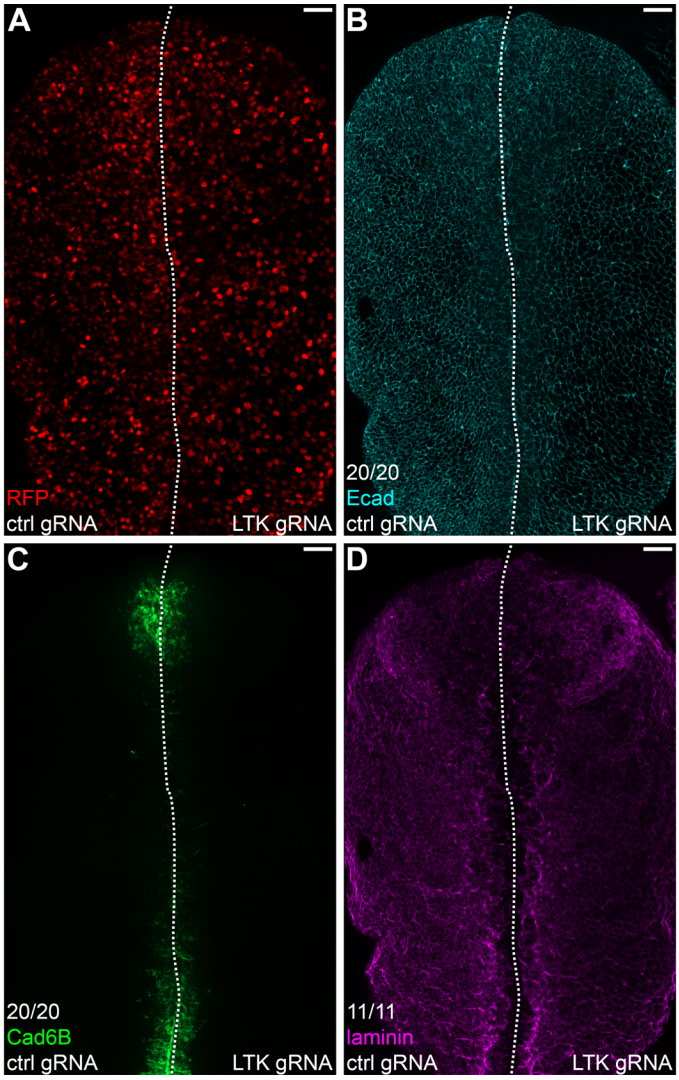

Figure S4. LTK is not required for epithelial to mesenchymal transition. (A-C) Immunostaining of HH10 embryos after unilateral CRISPR/Cas9-mediated depletion of LTK showing no obvious differences in the expression of Ecad (20 out of 20 embryos) (B), Cad6B (20 out of 20 embryos) (C) or laminin (11 out of 11 embryos) (D), suggesting no effects on EMT. RFP reporter was electroporated on both sides (A). Scale bars: 50 μm.

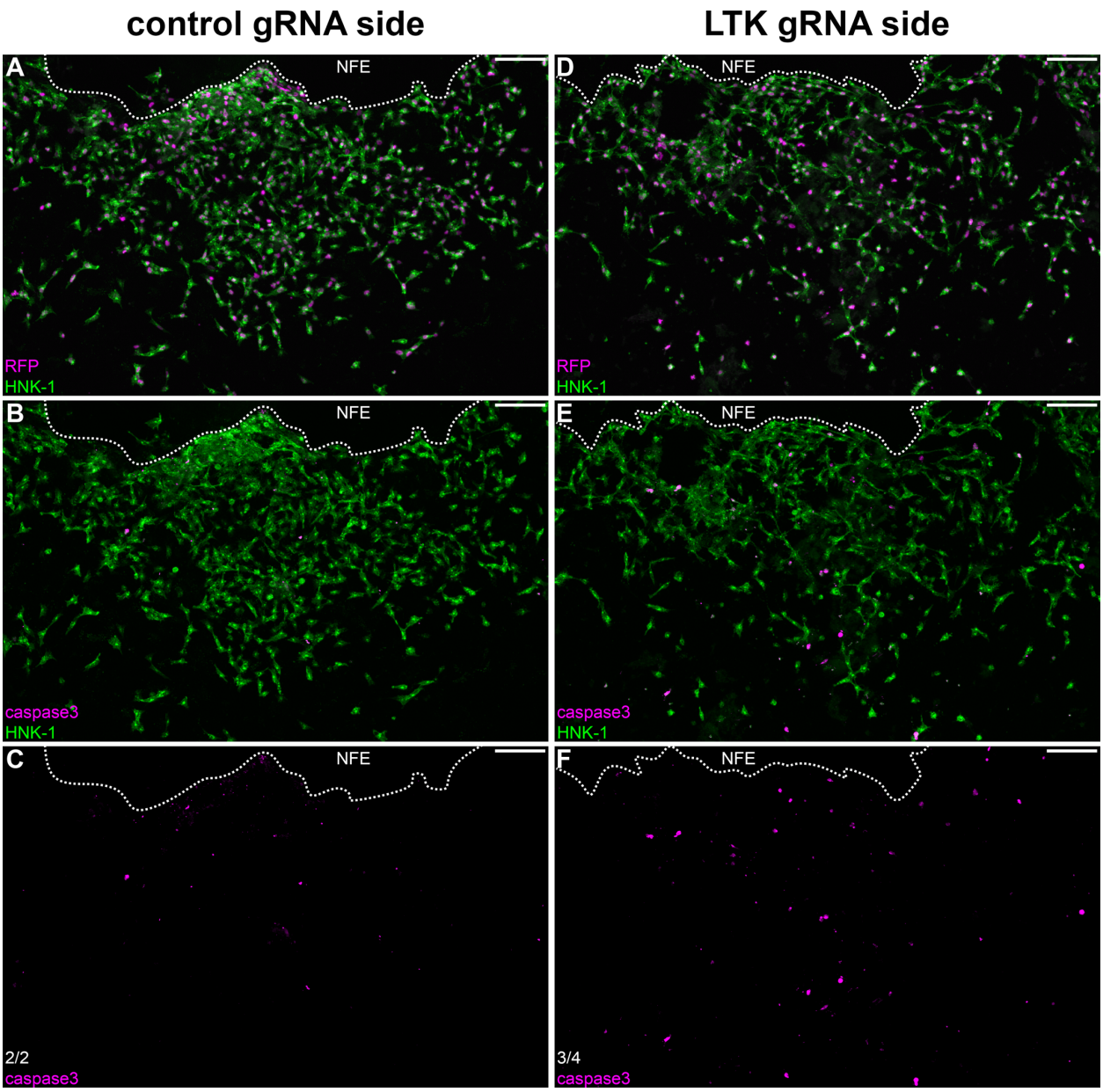

Figure S5. Loss of LTK mainly affects cell survival *in vitro*. (A-F) Immunostaining of HH8 neural fold explants obtained after unilateral CRISPR/Cas9-mediated depletion of LTK and cultured for 24 h showing that HNK-1^{+} neural crest cells delaminated and migrated from both control and experimental side explants (A-B,D-E), whereas LTK-depleted cells displayed higher levels of cleaved caspase3 in comparison to cells originating from the control explant, indicating increased cell death (C,F). RFP reporter and Cas9 were electroporated on both sides (A,D). NFE: neural fold explant. Scale bars: 100 μm.

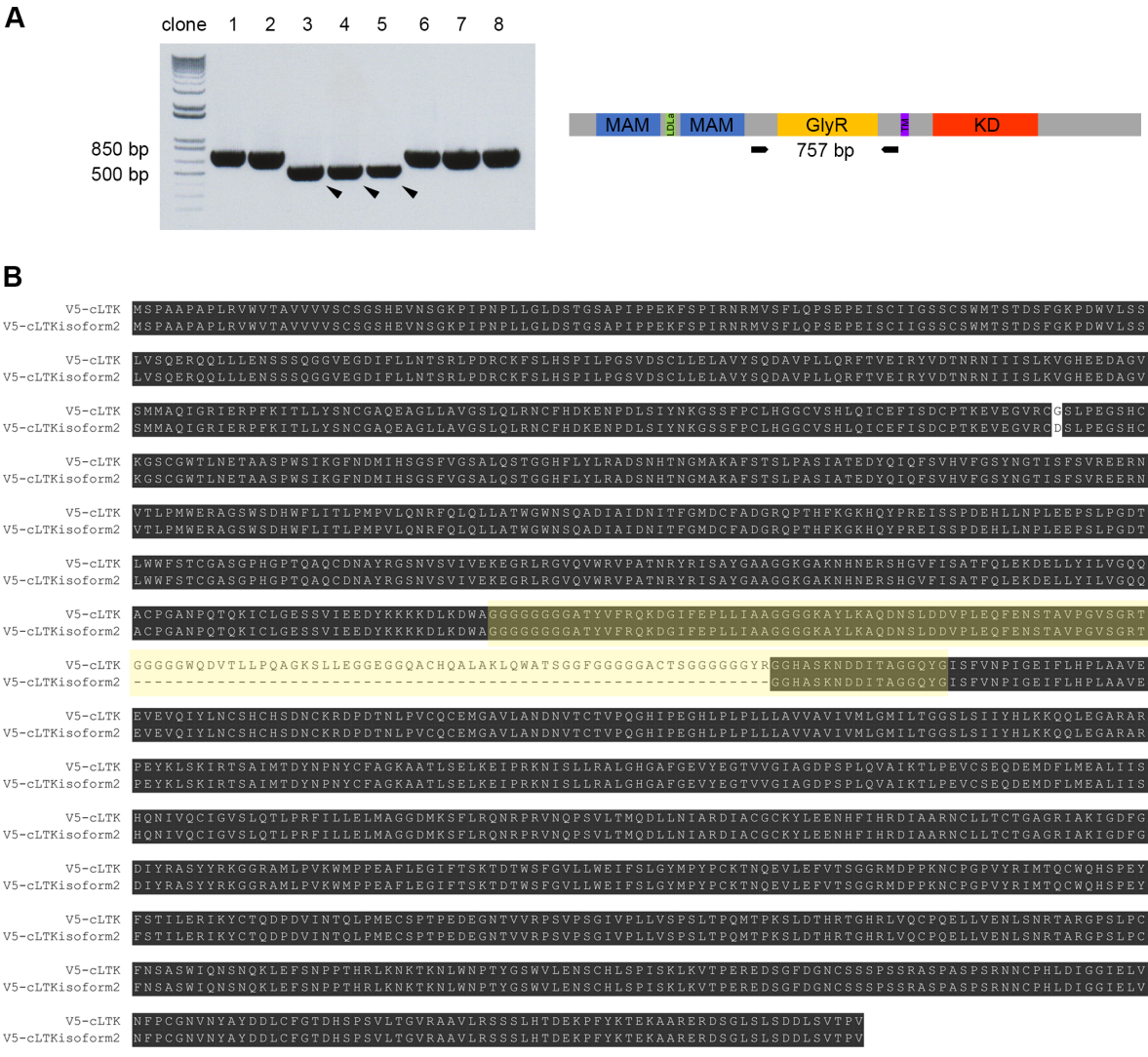

Figure S6. Predominant isoforms of LTK at stage HH10. (A) Gel image showing PCR products obtained after screening of bacterial clones transformed with plasmids resulting from ligation of full-length LTK obtained by RT-PCR from HH10 embryos, showing high frequency (3/8) of an isoform shorter than the predicted transcript (arrowheads). (B) Full-length sequence obtained for both isoforms revealed absence of exon 16 in the shorter isoform, predicting translation of an alternative protein product lacking significant portion of the GlyR domain (yellow shade).

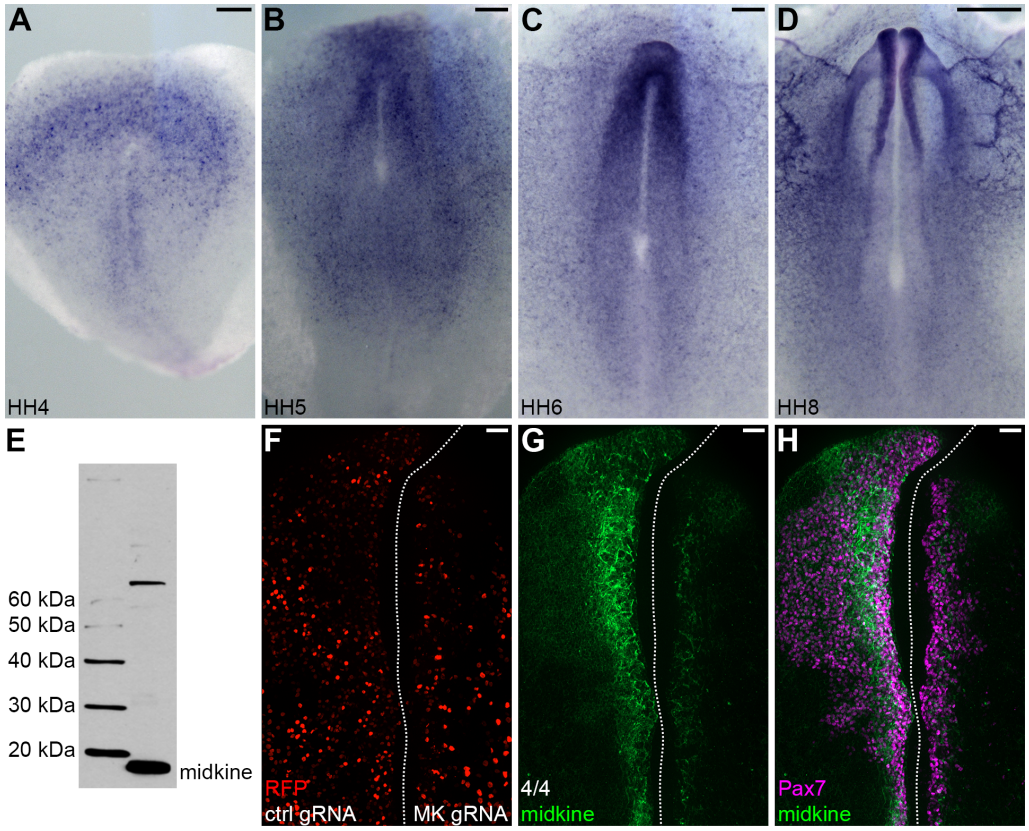

Figure S7. Expression of *midkine* during early chick development and validation of anti-midkine antibody and midkine gRNA used in this study. (A-C) *In situ* hybridization showing that *midkine* transcripts are expressed in the majority of the ectoderm at gastrulation stages HH4-6. (D) By HH8, midkine expression has been cleared from the central neural tube region but remains active in the neural folds. (E) Western blotting of lysates from heads of HH10 embryos with anti-midkine antibody allowed detection of a 15.5 kDa band, matching the predicted size for chicken midkine. (F-H) Unilateral CRISPR/Cas9-mediated depletion of midkine in gastrulating embryos (4 out of 4 embryos) (F) results in significant decrease of midkine protein by HH10 (G) and impaired neural crest migration (H). RFP reporter and Cas9 protein were electroporated on both sides (F). Scale bars: 200 μm in A-D; 50 μm in F-H.

Table S1. Primer sequences used in this work.

Primer	Sequence
FLAG_MK_R	TCATCGTCGTCTTTATAGTCCCCGCCACTACCACCGTCCTTCCCCTTGCCCTTCTTTGCT
FLAG_pCI_F	GCGGGGACTATAAAGACGACGATGATAAATGATAATCGAATTCCTGCAGCCCGGGGGATCCGCCCCT
LTK_F1	AGTCTCCCAGAGGGTTCACA
LTK_F2	GAGGGAGGTGCAGGAAAGCTAA
LTK_R1	TAGGCGTTGTCACACTGAGC
LTK_R2	TGTCCAGCCCAAGAACAGGTAG
MK_F1	ATGCAGCCCCGGGGCCTCCT
MK_R	GTCCTTCCCCTTGCCCTTCTTTGCTTTGG
MK_R1	GTCCTTCCCCTTGCCCTTCTTTGCTTTGG
pCAG_LTK_F	GCTCATCGATAAGCTTGATGCCACCATGAGCCCCGCTGCC
pCAG_LTK_R	CTGAGGAGTGAATTGCGGCCGCATCGATTATACTGGTGTAACACTCAAGTCATCTGACAG
pCAG_LTK_R2	CTGAGGAGTGAATTGCGGCCGCATCGATTATCTGGCTCCTTCCAGTTGCTG
pCI_LTK_R2	CCGGGCTGCAGGAATTCGATTCATTATCTGGCTCCTTCCAGTTGCTG
pCI_MK_F	AGCTCATCGATAAGCTTGATGCCACCATGCAGCCCCG
pCI_MK_F2	AGCTCATCGATAAGCTTGATGCCACCATGGCCAAAGCCAAGAAAGAGAAGATGA
V5_LTK_F	CCTATCCCTAACCCTCTCCTCGGTCTCGATTCTACGGGTTCTGCACCAATTCCTCCTGAG
V5_LTK_F2	CCTATCCCTAACCCTCTCCTCGGTCTCGATTCTACGGGTGGTCATGTCCCAGAGGGACAT
V5_LTK_R	GACCGAGGAGAGGGTTAGGGATAGGCTTACCAGAGTTTACTTCATGTGATCCAGAACAGG
V5_LTK_R2	GACCGAGGAGAGGGTTAGGGATAGGCTTACCTACTGGTGTAACACTCAAGTCATCTGACA